V European Conference on Computational Fluid Dynamics
ECCOMAS CFD 2010
J. C. F. Pereira and A. Sequeira (Eds)
Lisbon, Portugal, 14–17 June 2010

MODIFICATION AND EXTENSION OF A STANDARD VOLUME-OF-FLUID SOLVER FOR SIMULATING BOILING HEAT TRANSFER

Christian Kunkelmann[*], Peter Stephan[†]

[*]Institute of Technical Thermodynamics, Technische Universität Darmstadt
Petersenstraße 30, D-64287 Darmstadt, Germany
e-mail: kunkelmann@ttd.tu-darmstadt.de

[†]Institute of Technical Thermodynamics, Technische Universität Darmstadt
Petersenstraße 30, D-64287 Darmstadt, Germany
e-mail: pstephan@ttd.tu-darmstadt.de

Key words: volume-of-fluid, level-set, phase change, boiling heat transfer, contact line evaporation, bubble merger

Abstract. *In the present paper the modifications and extensions of the Volume-of-Fluid solver in the OpenFOAM CFD package for the simulation of boiling flows are presented. The main difficulties in the simulation of boiling flows are high temperature gradients at the liquid-vapor interface and microscopic heat and mass transfer at the 3-phase contact line. As the smeared interface in a pure Volume-of-Fluid method does not allow a precise reconstruction of the interface and thus hinders the accurate determination of the local temperature gradient, the solver is extended by a Level-Set method and a geometric reconstruction method. This facilitates an exact determination of the temperature gradient and of the local evaporation rate. In addition, the solver is extended by a sub-model for the microscale evaporation at the contact line which cannot be resolved on a CFD mesh. The sub-model is coupled to the simulation by adapting the thermal coupling between the solid heating wall and fluid domain. The modifications and the resulting model are validated by simulating phase change in a simple geometry and by simulating the heat and mass transfer during single bubble boiling. Further, the model is applied to perform a 3D simulation with adaptive mesh refinement of a lateral bubble merger. Very good qualitative and quantitative agreement with analytical approaches and experimental observations can be found.*

1 INTRODUCTION

Boiling is one of the most efficient ways to achieve high heat fluxes at a reasonable wall superheat. The high heat transfer coefficients that can be achieved are of utmost interest for many applications in the field of refrigeration, cooling of electronic devices as well as power generation. In a large number of applications, in particular cooling of high performance electronics, the devices become smaller while the heat dissipation and the maximum admissible temperature remain the same. Hence, the required heat transfer coefficients can easily exceed the ones that can be achieved with single phase heat transfer. Boiling can be an alternative, but there is need for accurate prediction of both heat transfer coefficient and critical heat flux. Unfortunately, many of the physical phenomena that occur in boiling and their interaction are still not well understood. Consequently, non-empirical predictive tools are rare.

The difficulties in both experimental and numerical investigations of boiling phenomena are due to the small length scales which have a non-negligible impact on the bubble growth (e. g. the microscale evaporation at the contact line), the highly dynamic nature of boiling heat transfer and the complexity of the transient heat transfer between solid, liquid and vapor. An accurate prediction tool for nucleate boiling in the isolated bubble regime has been developed by Fuchs et al. [1]. The model uses a Langrangian mesh that follows the motion of the liquid-vapor interface and captures the microscale heat transfer according to the work of Stephan and Busse [2]. The major drawbacks of the Lagrangian approach are the assumption that the bubble is spherical until it detaches from the heating wall and the incapability of the model to simulate interaction between multiple bubbles. In the past, very robust methods like Volume-of-Fluid (VOF) and Level-Set (LS) which can capture a moving interface on a fixed grid have been developed. Unfortunately, the modeling of phase change is more complex in such an approach because the position of the liquid-vapor interface does not coincide with a boundary of the computational domain. In a number of numerical works LS has been used to simulate boiling of water in different flow conditions (Son et al. [3]; Wu et al. [4]; Li and Dhir [5]). The authors found good agreement to experimental data. However, only boiling of water on isothermal heating walls was investigated. An approach for modeling phase change with VOF method is presented by Welch and Wilson [6] who simulated 1D test cases and film boiling. Unfortunately, no simulation was performed for boiling conditions. Kunkelmann and Stephan [7] implemented a boiling model into the CFD package OpenFOAM (Weller et al. [8]) and performed preliminary simulations for boiling of refrigerant HFE-7100. The model takes into account the transient heat conduction in the solid wall. Phase change is modeled according to the approach of Hardt and Wondra [9] which represents evaporation by smeared source terms in the conservation equations. Good qualitative agreement to high resolution measurements was found. One of the major drawbacks in the model of Kunkelmann and Stephan [7] is the high grid resolution that is required at the liquid-vapor interface. This requirement represents the bottleneck on the way towards 3D simulations of real boiling phenomena.

The aim of the present work is to show how a combination of VOF and LS can help to reduce the required mesh resolution at the interface. The boiling model, its sub-models and simulation results are presented and discussed. The growth of a spherical bubble in an infinitely extended superheated liquid is used to validate the phase change sub-model without contact line evaporation. In a next step, periodic single bubble boiling and the lateral merger of two bubbles growing at neighboring nucleation sites are investigated. The results are compared to high resolution experimental data in order to further validate the boiling model. Furthermore, the results permit a more detailed insight into the boiling process and can help to better understand the physical phenomena.

2 NUMERICAL METHOD

2.1 Governing equations of the overall model

The equations that need to be solved in the boiling model are the conservation equations for mass, momentum, energy and volume fraction:

$$\nabla \cdot (\rho \vec{u}) = \dot{\rho} \tag{1}$$

$$\frac{\partial \rho \vec{u}}{\partial t} + \nabla \cdot (\vec{u} \cdot \rho \vec{u}) = -\nabla p + \nabla \cdot (\mu \cdot \nabla \vec{u}) + \vec{f}_{ST} + \vec{f}_g \tag{2}$$

$$\frac{\partial \rho c T}{\partial t} + \nabla \cdot (\vec{u} \cdot \rho c T) = \nabla \cdot (\lambda \cdot \nabla T) + \dot{h} \tag{3}$$

$$\frac{\partial F}{\partial t} + \nabla \cdot (\vec{u} \cdot F) = \frac{\dot{\rho}}{\rho} F \tag{4}$$

The volume fraction field F determines the liquid volume fraction in each cell. It has a value of 0 in vapor cells, a value of 1 in liquid cells and a value in between in the cells that contain the liquid-vapor interface. The volumetric forces $\vec{f}_{ST}$ and $\vec{f}_g$ on the right hand side of Eq. (2) account for surface tension and gravity, respectively, while the source terms on the right hand sides of Eqs. (1), (3) and (4) account for the phase change. The calculation of the source term field is explained below. Mass is removed on the liquid side of the interface and reappears on the vapor side. In spite of the local mass source terms, the mass is globally conserved.

In each time step, the following tasks are performed by the solver:

1. Advection of VOF field
2. Calculation of LS field and reconstruction of liquid-vapor interface
3. Solution of energy equation in an iterative sub-cycle:
   a. Calculation of evaporation rate at the liquid-vapor interface
   b. Calculation of contact line evaporation
   c. Exchanging boundary conditions at solid-fluid interface
   d. Solving energy equation in solid and fluid
4. Solution of pressure-velocity coupling (PISO algorithm)

In the following the sub-models for interface reconstruction, phase change and contact line evaporation will be discussed.

2.2 Interface reconstruction

In boiling conditions the temperature profile in vicinity of the liquid-vapor interface is changing tremendously in a very narrow space. The discussion of the test case in the following section provides more quantitative information on this difficulty. As the temperature gradient on the liquid side of the interface controls the local rate of phase change, it is required to resolve this value as accurate as possible. Additionally, the exact position of the 3-phase contact line must be known for the contact line evaporation. In the VOF approach that is implemented in OpenFOAM the interface is typically smeared over two to three mesh cells (see Figure 1). This leads to an inaccuracy regarding the exact position of the interface. Consequently, the temperature gradient and the contact line evaporation cannot be calculated accurately. In a previous publication [7], the authors used a pure VOF approach and could overcome the problem with a very fine mesh. However, such a fine mesh cannot be used for 3D simulations. Therefore, the precise interface position has to be obtained even on coarse

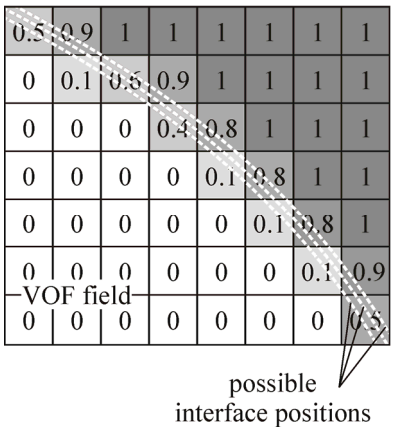

Figure 1: Smeared interface in VOF method and resulting uncertainty on interface position.

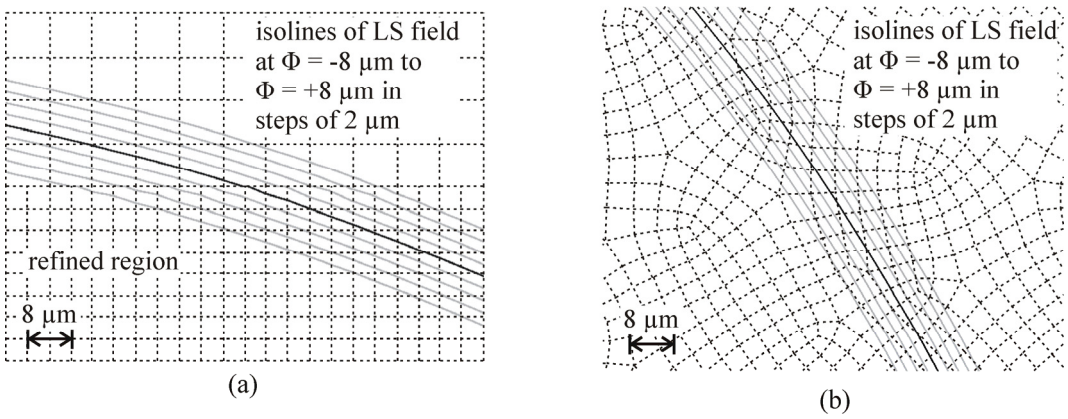

Figure 2: Isolines of calculated LS field on (a) a grid with a step in resolution and (b) an unstructured grid.

grids. An approach that provides more precise information about the interface position is the LS method. In spite of using a complete LS method, a coupling between VOF and LS is implemented allowing an exact interface reconstruction while keeping the robustness of VOF. In the resulting model, no transport equation is solved for the LS field but it is calculated from the VOF field in every time step. First, the LS field is guessed from the VOF field:

$$\Phi = \left(2 \cdot F - 1\right) \cdot \varepsilon \tag{5}$$

This step results in a signed field that has a value of 0 at the interface, $+\varepsilon$ in the liquid phase and $-\varepsilon$ in the vapor phase. In order to obtain a signed distance field, the estimated field is corrected according to the approach of Sussman et al. [10]:

$$\frac{\partial \Phi}{\partial \tau} + \vec{w} \cdot \nabla \Phi = \operatorname{sign}\left(\Phi\right) \tag{6}$$

$$\vec{w} = \operatorname{sign}\left(\Phi\right) \cdot \frac{\nabla \Phi}{\left|\nabla \Phi\right|} \tag{7}$$

The correction is primarily acting in a band close to the interface. As the distance information is needed only in vicinity of the interface, very little iteration is required. This method is very robust and provides good results even on meshes with steps in resolution and unstructured, non-orthogonal meshes (see Figure 2).

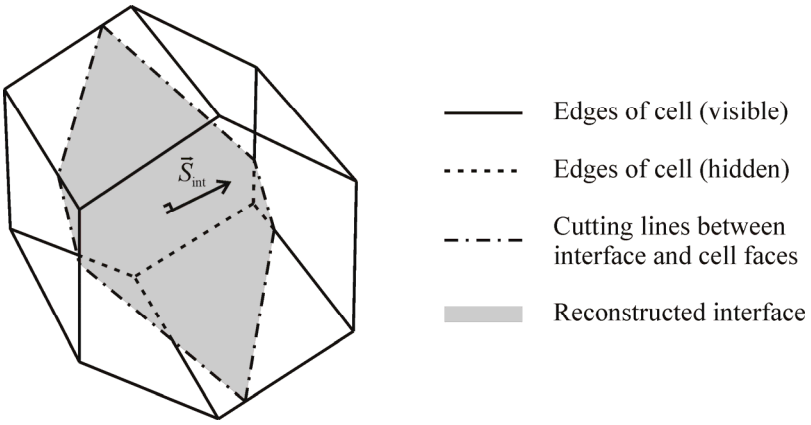

Figure 3: Geometric reconstruction of the interface in a polyhedral cell.

Once the LS field has been calculated, the interface can be reconstructed in each cell. According to the method of López and Hernández [11], this is done by geometrically cutting the cell with the interface. The cutting lines between the cell faces and the interface form the segment of the interface in the cell (see Figure 3). Although the implementation of this method of reconstruction requires a significant implementation effort, it has been chosen for the boiling model as it is not limited to hexagonal or orthogonal meshes.

2.3 Phase change

Apart from the very early stage of bubble growth which is not subject of the present paper, the interface can be assumed to be in thermodynamic equilibrium. The temperature at the interface is therefore equal to the saturation temperature that corresponds to the pressure level. Furthermore, the heat transfer in the vapor phase can be regarded as very small compared to the heat transfer in the liquid phase. Therefore, the interface and the vapor are assumed to be at saturation temperature. Under these conditions, the evaporation rate (in $\mathrm{kg\,s^{-1}\,m^{-3}}$) at the interface can be calculated in every cell:

$$\dot{\rho}_{0,i} = \frac{\lambda_l \cdot \nabla T \cdot \vec{S}_{\text{int},i}}{h_{lv} V_i} = \frac{\lambda_l \cdot \left(T_i - T_{sat}\right) \cdot S_{\text{int},i}}{h_{lv} \Phi_i V_i} \tag{8}$$

The resulting field is localized at the interface. Instead of imposing a volume expansion due to phase change in the interface cells, the method of Hardt and Wondra [9] is used to smear the source term field. After removing the source terms in the interface cells, the source term field is rescaled in the liquid and the vapor phase according to the original rate of phase change. This approach permits to divide the source terms into mass sinks (liquid side) and sources (vapor side) and results in a very robust implementation of phase change.

2.4 Contact line evaporation

The microscale heat transfer at the contact line is governed by physics that act on a length scale which cannot be resolved by the numerical mesh. Therefore, the contact line heat transfer has to be treated by a sub-model that interacts with the simulation. In a microscopic scale there is no actual contact line, as illustrated in Figure 4a. In the adsorbed film region liquid molecules are attracted by adhesion forces and stick to the wall without evaporating. These forces are negligible in the macro region. The adsorbed film and the macro region are connected by the micro region. Stephan and Busse [2] derive a fourth order differential equation for this region which can be solved numerically. The results (film thickness, curvature, heat flux and integrated heat flux) are shown exemplarily in Figure 4b. For a given fluid the results depend mainly on the wall superheat and can be correlated prior to the

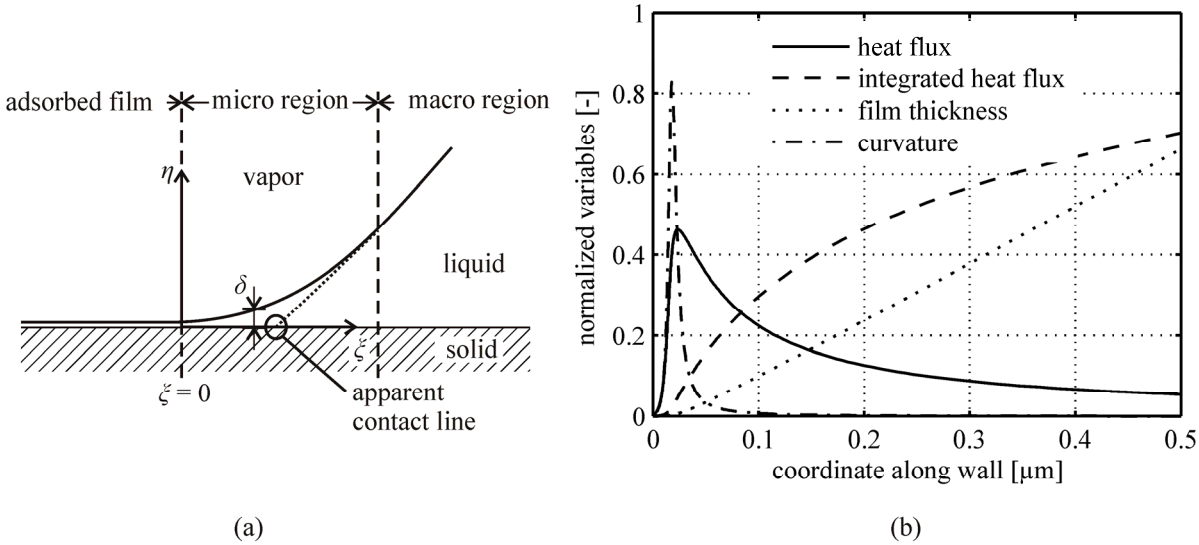

Figure 4: (a) Microscopic contact line region; (b) development of heat flux (normalized by 50 MWm^{-2}), integrated heat flux (normalized by 5 Wm^{-1}), film thickness (normalized by 0.5 μm) and curvature (normalized by 50 μm^{-1}) in the micro region (results for refrigerant HFE-7100 at 500 mbar, 15 K wall superheat).

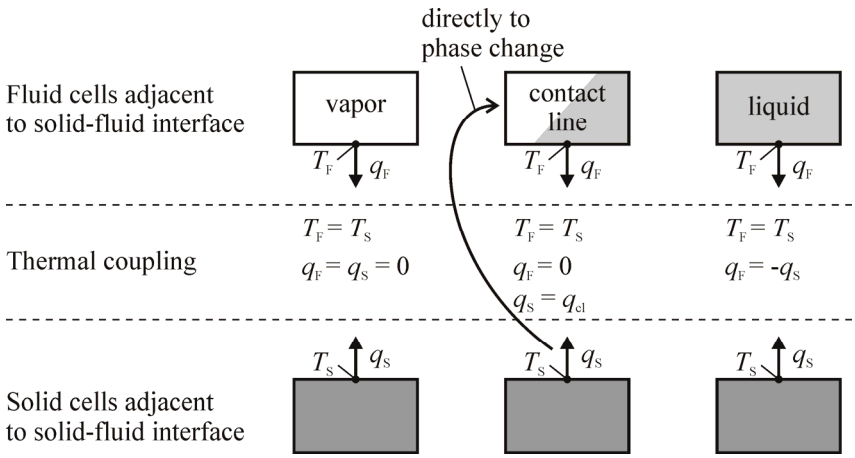

Figure 5: Different thermal coupling at the solid-fluid interface for cells containing pure vapor, cells containing the contact line and cells containing pure liquid.

simulation. The most important parameters for coupling the sub-model to the simulation is the integrated heat flux (heat flow per unit contact line length) and the local wall superheat at the contact line. The local wall superheat is taken from the simulation and serves as input parameter for the sub-model. The sub-model calculates the integrated heat flux which is then multiplied by the contact line length in the cell and used as a boundary condition in the simulation.

The interface reconstruction can also be used to reconstruct the contact line in the cells that are adjacent to the solid-fluid interface. While the local heat flux in cells without contact line is a result of the thermal coupling between solid and fluid, the local heat flux in cells containing a part of the contact line is determined from the local wall superheat according to the above mentioned correlation from the contact line sub-model. In cells with contact line, the heat flux on the fluid side is set to zero and the heat transfer from the wall directly enhances phase change. The different situations are illustrated in Figure 5.

3 SIMULATION RESULTS

3.1 Growth of a spherical bubble in superheated liquid

As a first test case the growth of a spherical vapor bubble in an infinitely extended superheated liquid is simulated. Due to the fact that there is no contact line this case is less complex than the real boiling process. An analytical solution for this case has been presented by Scriven [12]. The existence of an analytical solution allows validating the phase change model. Simulations have been performed for refrigerant HFE-7100 at a pressure of 500 mbar. Different liquid superheats (5 and 10 K) and different mesh resolutions (1, 2 and 4 µm) were applied. Bubbles with an initial radius of 0.1 mm were placed into superheated liquid. The initial temperature profile in vicinity of the interface is taken from the analytical solution at the instance corresponding to the initial bubble size. This profile describes the temperature drop from superheated conditions in the bulk liquid to saturation temperature at the interface. Depending on the superheat, the temperature drop in vicinity of the interface takes place on a length of only 6.8 µm (5 K superheat) and 3.3 µm (10 K superheat). It is obvious that a rather fine grid is required at the interface to resolve this temperature drop.

The growth of the bubble radius with time is shown in Figure 6. The numerical results are in very good agreement to the analytical solution. With finer mesh resolution the results converge towards the analytical solution. Compared to the results that were obtained by the authors in a previous study [7] for a superheat of 5 K without LS method and geometric interface reconstruction, the extensions allow using a significantly coarser mesh (2 µm instead of 0.5 µm) without decreasing the level of accuracy. Hence, the sub-model for interface reconstruction and phase change are validated. In addition, the test case shows that the extension of the pure VOF method pays off due to a significant reduction of the required mesh size. This amelioration of the phase change model is absolutely required for the 3D simulation of boiling flows which is one of the aims of the model development.

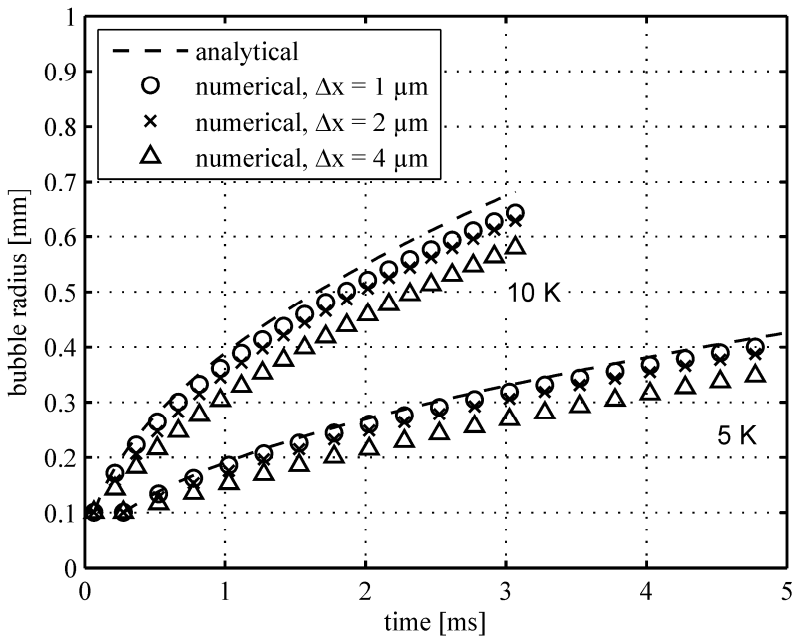

Figure 6: Growth of spherical vapor bubble in infinitely extended superheated liquid; development of bubble radius with time.

3.2 Periodic single bubble boiling

The high complexity of boiling heat transfer does not allow an analytical approach as in the case presented before. Therefore, the complete model including contact line evaporation must be validated by comparing simulation results to experimental data. A generic experimental setup with well defined boundary conditions and highly resolved data acquisition has been used by Wagner et al. [13]. The authors investigated boiling of refrigerant HFE-7100 at 500 mbar on a steel heating foil with a thickness of 50 µm. An artificial nucleation site on the heating foil enabled the generation of single bubbles at a prescribed position. The steel foil is heated by an electric current resulting in a heat flux of 5400 Wm^{-2}. The bubble shape is observed with a high speed camera from the side, while the temperature of the steel heating foil was measured with a high speed infrared camera from below. The authors observe periodic bubble events with a bubble growth time of 13 ms and a departure diameter of 1.9 mm. The mean superheat of the heating foil is around 15 K. The

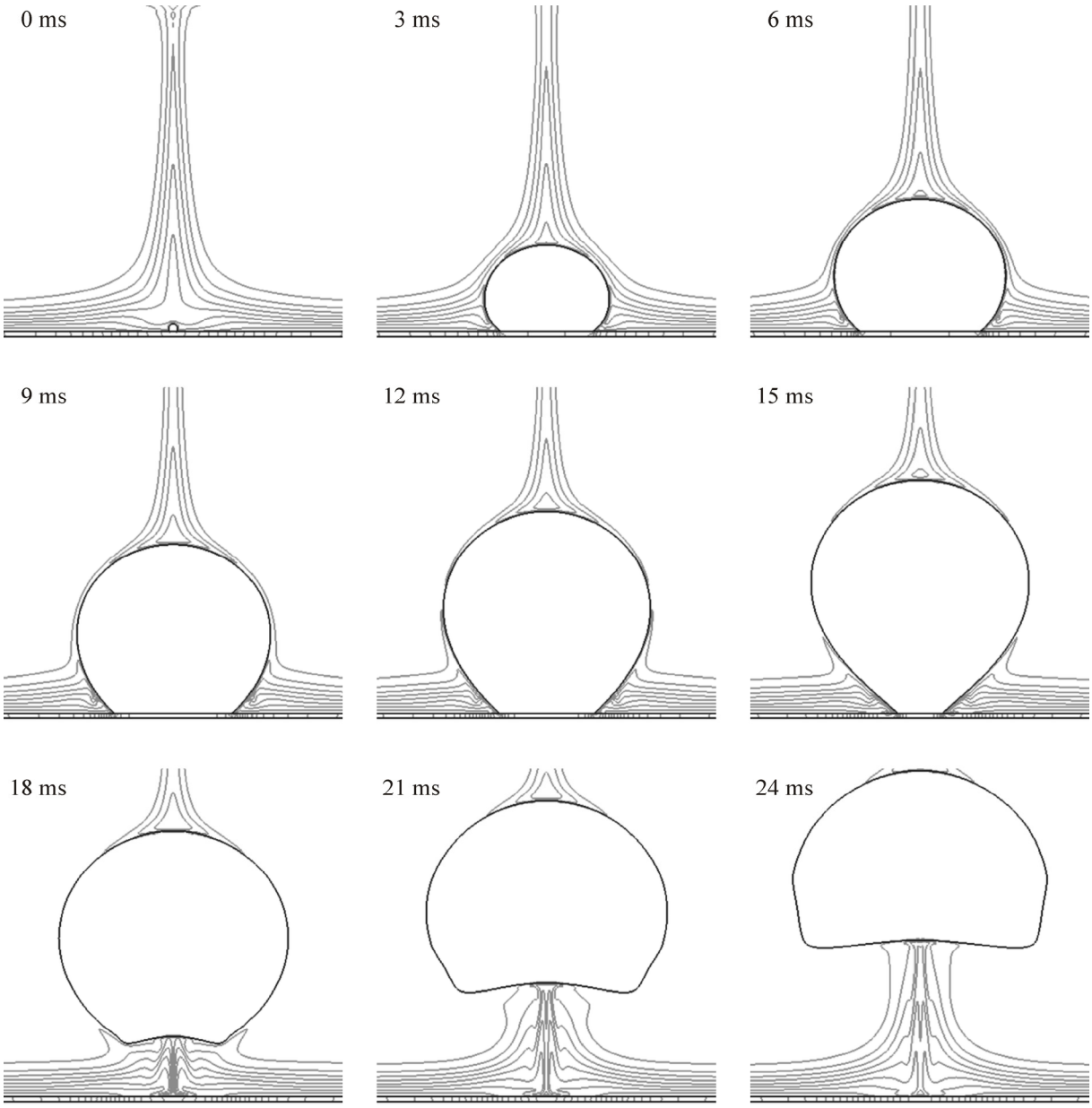

Figure 7: Bubble contour and isotherms during one bubble cycle (temperature step between isotherms: 2 K in liquid, 0.2 K in solid).

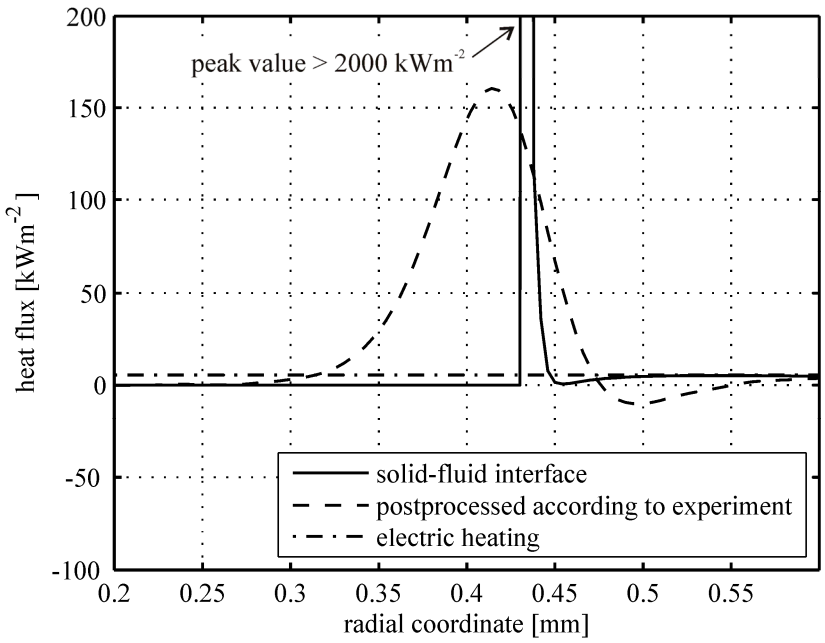

Figure 8: Heat flux peak at the 3-phase contact line 3 ms after nucleation (direct boundary field at solid-fluid interface and postprocessed according to experiment) and constant heat flux from electric heating.

high temporal and spatial resolutions of the experimental apparatus allow observing the local cooling and the high local heat fluxes at the contact line. At the contact line the authors measure a temperature decrease of about 1.5 K and a local heat flux peak of about 150 kWm^{-2}. The authors state that 20 – 30 % of the total heat consumed by the bubble is transferred in the near contact line region.

In the following, the setup of the simulation is explained and its results are shown and compared to experimental data. Initially, the temperature profile in the liquid layer close to the heating wall is assumed to be linear with a thickness of 0.18 mm while the heating wall is assumed to have an initial constant superheat of 15 K. These choices are arbitrary, but the simulation of several consecutive bubble cycles permits to reach a periodic regime which is independent of the initial conditions. In Figure 7 the bubble shape and the temperature field during a complete bubble cycle in the periodic regime are shown. Departure diameter, growth time and mean wall temperature converge to values which are a little above the values observed in the experiment (see Table 1). However, due to the high complexity of boiling, the results are very satisfying. The deviations in departure diameter and growth time are most probably due to the assumption of a static contact angle. A contact angle of 40° has been chosen according to the experimental observations of the bubble shape. However, the contact angle is most probably changing dynamically during bubble growth and detachment. This simplification certainly influences departure diameter and the growth time.

	Experiment [13]	**Simulation**
Departure diameter	1.9 mm	2.3 mm
Growth time	13 ms	16 ms
Mean wall superheat	15 K	16.5 K
Maximum heat flux at contact line (postprocessed as in experiment)	150 kWm^{-2}	160 kWm^{-2}
Temperature drop at contact line	1.5 K	1.5 K
Ratio of heat transferred near contact line	20 – 30 %	20 – 25 %

Table 1: Quantitative comparison between experiment [13] and simulation.

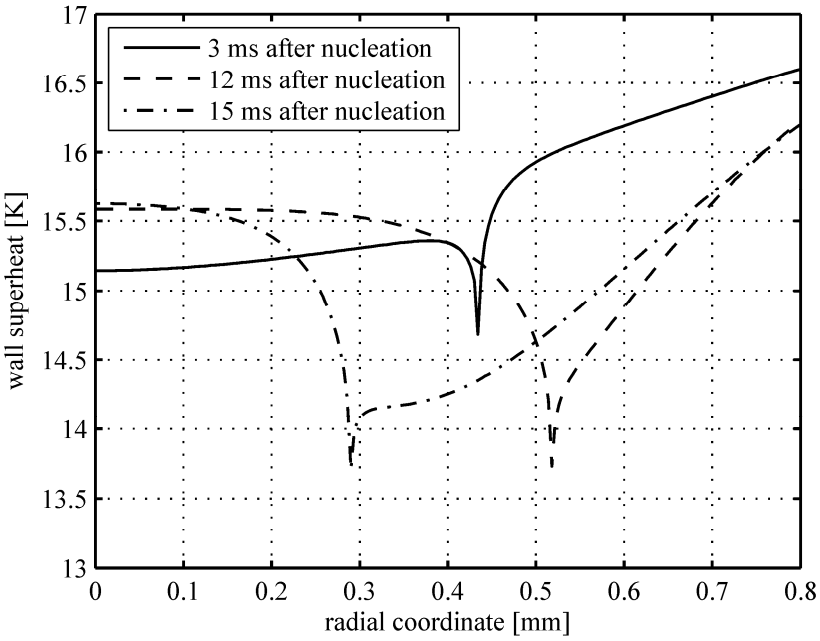

Figure 9: Local minimum of wall temperature at the contact line for receding (3 ms), stagnating (12 ms) and advancing (15 ms) contact line.

In order to validate the contact line sub-model, the local heat flux at the position of the contact line is compared to experimental observations. In the experiment, the local heat flux is calculated via an energy balance from the high speed IR images of the heating foil's back side. In the simulation, the heat flux can be obtained from at the actual solid-fluid interface or by imitating the experimental data processing. In the second case, smearing and shifting of the heat flux peak due to the thickness of the heating foil is observed (see Figure 8). The value of the maximum heat flux is in very good agreement to the experiment (see Table 1) and quantifies the signal damping in the heating foil. The high heat flux at the contact line leads to a local cooling of the wall. The temperature drop at different instances can be seen in Figure 9. Again, the value of around 1.5 K is in good agreement to the experiment (see Table 1). The simulation results also support the experimental observation that a significant part (20 – 25 %) of the total heat consumed by the bubble is transferred in the near contact line region.

3.3 Lateral bubble merger

The implementation of the LS method and the resulting reduction of the required mesh resolution enable the 3D simulation of boiling phenomena. In order to demonstrate the capabilities of the boiling model to provide detailed insight and to enhance understanding of the physics of boiling, the lateral merger of two bubbles is simulated. According to the measurements performed by Wagner [14] two bubbles are assumed to grow at neighboring nucleation sites with a distance of 1 mm. In addition to the boiling model, an adaptive mesh refinement algorithm is used to account for the high grid resolution required at the interface. The refinement regions are defined by a critical distance to the interface. Three refinement steps are used and result in a mesh size of 4 µm in the refined regions (see Figure 10). Thus, the total number of cells is moderate and remains between 0.5 and 2 million cells, depending on the bubble size.

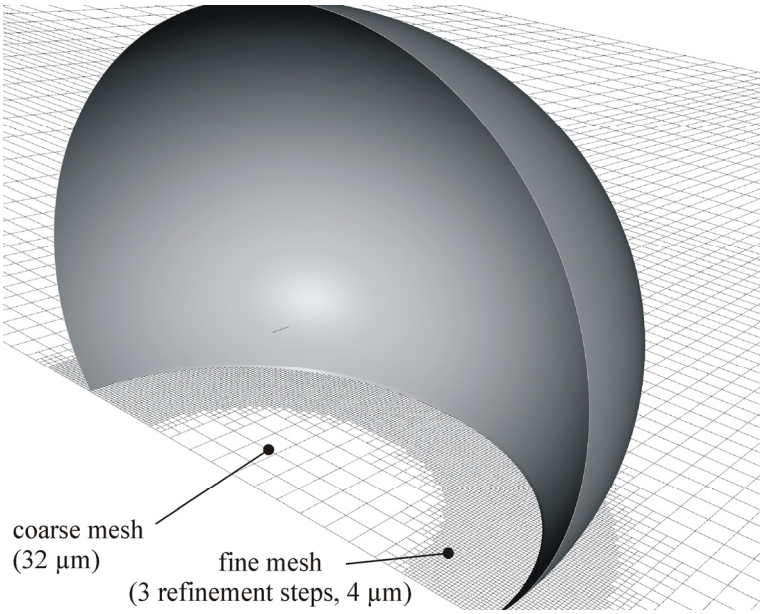

Figure 10: Illustration of adaptive mesh refinement in vicinity of the liquid-vapor interface for the simulation of a lateral bubble merger.

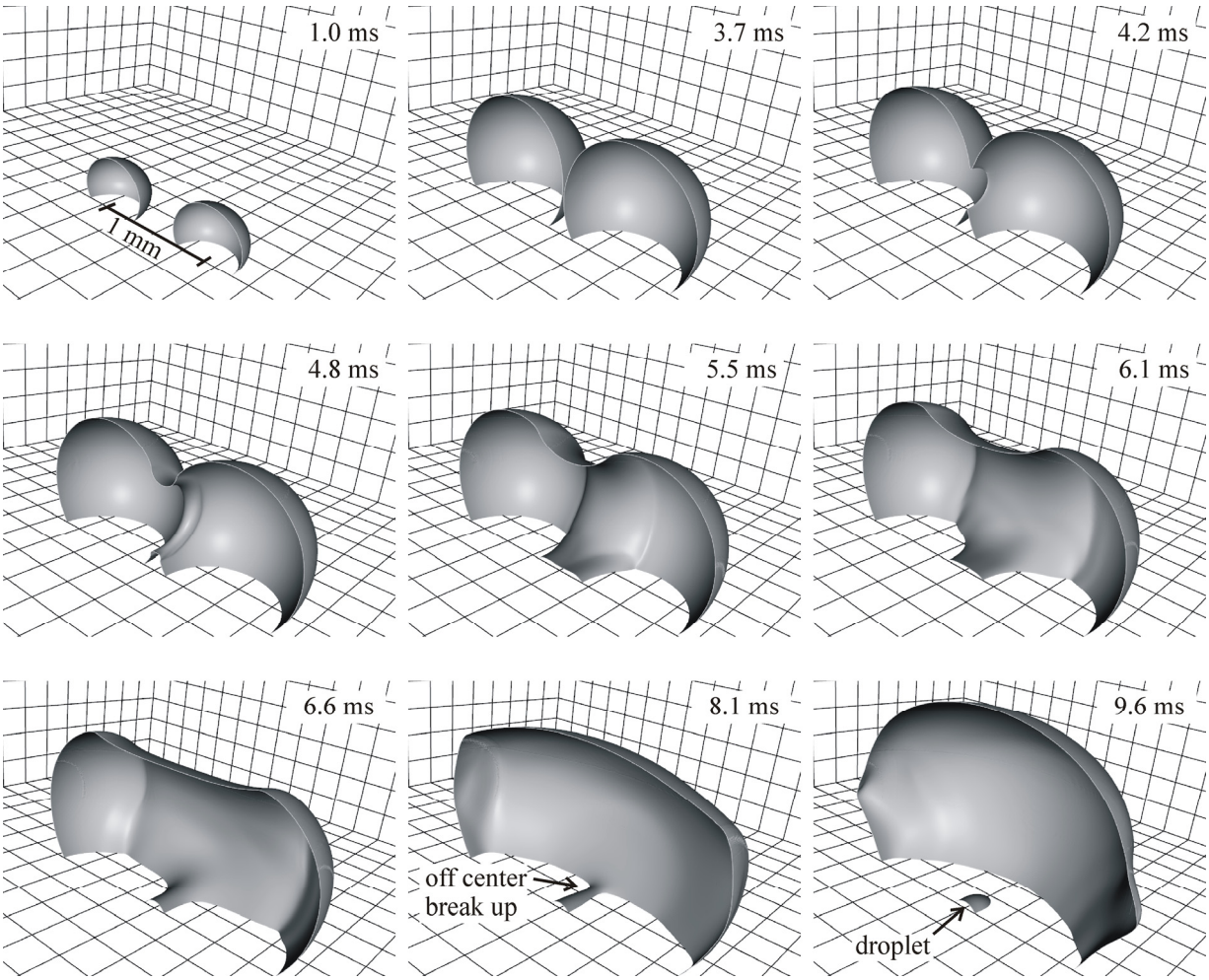

Figure 11: Bubble shape during a lateral bubble merger; formation of a droplet inside the merged bubble.

The bubble shape during the process of coalescence is shown in Figure 11. Interestingly, the liquid underneath the vapor bridge does not break up at a single point in the center between the bubbles. Instead, break up happens at two points with some offset from the center between the bubbles. Thus, a droplet is created that sits on the heater inside the merged bubble. The formation of droplets inside the merged bubble during boiling of refrigerants was observed experimentally by Wagner [14]. In another study incorporating numerical and experimental results (Mukherjee and Dhir [15]) the formation of droplets is not observed in the case of a lateral merger between two bubbles during boiling of water. However, this difference can probably be explained by the lower surface tension of HFE-7100 compared to water. The lower surface tension forces are too weak to completely push the liquid away from the center between the two bubbles.

4 CONCLUSION

In the present paper the numerical challenges of boiling simulations are shown and numerical methods that allow overcoming these challenges are presented. The difficulties are in particular due to high temperature gradients at the liquid-vapor interface which cannot be resolved in a pure VOF method and microscale evaporation at the contact line which is governed by physics that act on length scales that cannot be resolved by the CFD mesh. In order to allow for an accurate calculation of the temperature gradients at the liquid-vapor interface, the LS method together with a geometric reconstruction of the interface is coupled to the VOF solver of the OpenFOAM CFD package. This extension enables an exact determination of the interface position and in consequence of the temperature gradient. The implementation of the LS method and the interface reconstruction is very robust and can be applied even for general polyhedral meshes. In a test case with a simple geometry the model could be validated and proves to pay off by reducing the required mesh resolution. Compared to the model without LS method and interface reconstruction, the cell size could be increased by a factor of four without loosing accuracy. The evaporation at the 3-phase contact line is treated by a sub-model that accounts for the physics in the microscopic transition region between adsorbed film and macroscopic bubble shape. The coupling between the sub-model and the CFD simulation is done by locally adapting the conjugate heat transfer between the solid and the fluid domain. The complete model is applied to simulate the growth and detachment of single bubbles on a thin heating foil according to a high resolution experiment. The results are compared globally via departure diameter, growth time and mean wall temperature as well as locally via the heat flux and the temperature drop at the contact line. The results are in good quantitative agreement and prove the physical correctness of the model. For some parameters like departure diameter and growth time the rather large difference between experimental data and simulation is probably due to the assumption of a static contact angle. In a last step, the lateral merger of two bubbles growing at neighboring nucleation sites is simulated. The adaptive mesh refinement algorithm of the OpenFOAM CFD package is applied to make the simulation possible at a reasonable computational effort. The results are very promising and an interesting effect, namely the formation of a droplet inside the merged bubble, can be reproduced. For the used refrigerant, this effect has also been observed experimentally. Hence, the model has proven to be capable of correctly predicting very complex boiling flows and to facilitate a more comprehensive understanding of the complex heat and mass transfer in boiling.

REFERENCES

[1] T. Fuchs, J. Kern and P. Stephan, A transient nucleate boiling model including micro-scale effects and wall heat transfer, *J. Heat Transfer* **128**, pp. 1257-1265 (2006)

[2] P. C. Stephan and C. A. Busse, Analysis of the heat transfer coefficient of grooved heat pipe evaporator walls, *Int. J. Heat Mass Transfer* **35**, pp. 383-391 (1992)

[3] G. Son, V. K. Dhir and N. Ramanujapu, Dynamics and heat transfer associated with a single bubble during nucleate boiling on a horizontal surface, *J. Heat Transfer* **121**, pp. 623-631 (1999)

[4] J. Wu, V. K. Dhir and J. Qian, Numerical simulation of subcooled nucleate boiling by coupling level-set method with moving-mesh method, *Numer. Heat Transfer B* **51**, pp. 535-563 (2007)

[5] D. Li and V. K. Dhir, Numerical study of single bubble dynamics during flow boiling, *J. Heat Transfer* **129**, pp. 864-876 (2007)

[6] S. W. J. Welch and J. Wilson, A volume of fluid based method for fluid flows with phase change, *J. Computational Physics* **160**, pp. 662-682 (2000)

[7] C. Kunkelmann and P. Stephan, CFD simulation of boiling flows using the volume-of-fluid method within OpenFOAM, *Numer. Heat Transfer A* **56**, pp. 631-646 (2009)

[8] H. G. Weller, G. Tabor, H. Jasak and C. Fureby, A tensorial approach to computational continuum mechanics using object-oriented techniques, *Computers in Physics* **12**, pp. 620-631 (1998)

[9] S. Hardt and F. Wondra, Evaporation model for interfacial flows based on a continuum-field representation of source terms, *J. Computational Physics* **227**, pp. 5871-5895 (2008)

[10] M. Sussman, A. S. Almgren, J. B. Bell, P. Colella, L. H. Howell and M. L. Welcome, An adaptive level set approach for incompressible two-phase flows, *J. Computational Physics* **148**, pp. 81-124 (1999)

[11] J. López and J. Hernández, Analytical and geometrical tools for 3D volume of fluid methods in general grids, *J. Computational Physics* **227**, pp. 5939-5948 (2008)

[12] L. E. Scriven, On the dynamics of phase growth, *Chem. Eng. Sci.* **10**, pp. 1-13 (1959)

[13] E. Wagner, P. Stephan, O. Koeppen and H. Auracher, High resolution temperature measurements at moving vapor/liquid and vapor/liquid/solid interfaces during bubble growth in nucleate boiling, In proceedings of the 4th International Berlin Workshop on Transport Phenomena with Moving Boundaries, IBW4 2007, Berlin, Germany, pp. 260-277 (2007)

[14] E. Wagner, Hochauflösende Messungen beim Blasensieden von Reinstoffen und Gemischen, Dissertation, *Shaker Verlag* (2009)

[15] A. Mukherjee and V. K. Dhir, Study of lateral merger of vapor bubbles during nucleate pool boiling, *J. Heat Transfer* **126**, pp. 1023-1039 (2004)